Research Journal of Applied Sciences, Engineering and Technology 11(3): 259-266, 2015
DOI: 10.19026/rjaset.11.1715
ISSN: 2040-7459; e-ISSN: 2040-7467

Submitted: November 25, 2014 Accepted: January 8, 2015 Published: September 25, 2015

Research Article

Fusion of SAR Images for Improved Classification of Flooded Areas in the Northern Peninsular Malaysia

[1]Hafsat Saleh Dutsenwai, [2]Baharin Bin Ahmad, [3]Abubakar Mijinyawa and [4]Khamaruzaman B. Wan Yusof
[1]Department of Remote Sensing, Faculty Geoinformation and Real Estate, Universiti Technologi Malaysia, UTM,
[2]Department of Geoinformation, Faculty Geoinformation and Real Estate, Universiti Technologi Malaysia, UTM,
[3]Department of Geoscience and Petroleum Engineering, Universiti Technologi PETRONAS, UTP,
[4]Department of Civil Engineering, Universiti Technologi PETRONAS, UTP, Malaysia

Abstract: The northern peninsular of Malaysia has lost a lot of lives and property worth billions to the series of floods that have been occurring for many years. Many disaster management strategies have been adopted by the Malaysian government in handling these flood disasters but it is still a topic in the annual agenda. This research project aimed at using fusion techniques in order to obtain more interpretable information and boundaries in classification of SAR images which can aid in addressing the flood disastrous challenges in the study area. This was achieved through the fusion of two Radarsat-1 images and a TerraSAR-X image of the study area and secondly by investigation of a suitable fusion technique for delineation of flooded areas in the study area. The techniques used include the Hue Saturation and Value (HSV), the Brovey Transformation (BT), the Gram Schmidt (GS) and the Principal Component Spectral Sharpening (PCSS), which were classified using Maximum Likelihood (ML) and support Vector Machine (SVM). The results indicated that BT is the most suitable among all the fusion techniques used having the highest overall accuracy of 70.9615% and kappa coefficient of 0.3418.

Keywords: Classification, disastrous, flood, fusion, SAR

INTRODUCTION

The frequency, tendency and magnitude of natural disasters increase simultaneously with the rapid global increase (Lawal *et al*., 2011). Disasters such as floods, earthquakes, volcanic eruptions, tornadoes and landslides are persistently causing setbacks in mostly developing and even the developed nations, killing millions of people and destroying high amount of dollars annually (Lawal *et al*., 2013). Many countries have experienced loss of lives, injuries and destruction of property and significant fall in socioeconomic well being due to natural hazards occurrences. According to the Federal Emergency Management Agency (FEMA) of the USA, floods are one of the most typical and prevalent natural disasters, killing an average of over 225 people accompanied by loss of property that worth over USD3.5 billion due to smashing up by severe rainfall along with annual flooding (FEMA, 2014).

Floods are regarded as the most severe type of disaster encountered in Malaysia (Chan 2012a; Varikoden *et al*., 2011; Toriman *et al*., 2009b). Malaysia has experienced different climatic and weather events including El Nino 1997 and La Nina in 2011 and 2012, leading to severe droughts and floods respectively. Both cases of flash and monsoonal floods are experienced including other natural disasters such as landslides and haze, causing heavy life and property loss and the deterioration of the quality of air (Chan, 2012a). The monsoonal floods which occur annually vary in terms of pace, severity and time of occurrences, with the 2010 flood of Kedah and Perlis listed among the worst floods that the country has ever encountered (Chan, 2012a).

According to the Department of Irrigation and Drainage (DID) Malaysia, around 29000km of the total land area and over 22% of individuals are affected by floods yearly, accompanied by damages accounting for an approximate amount of about RM915 million (Toriman *et al*., 2009b). Flash floods are typical in Malaysia and a significant number of urban areas encountered this type of floods, which usually occur during the time of monsoon, for example the North-East monsoon from November to March and the South-

Corresponding Author: Baharin Bin Ahmad, Department of Geoinformation, Faculty Geoinformation and Real Estate, Universiti Technologi Malaysia, UTM, Malaysia

Fig. 1: Study area

West Monsoon from May to September (Toriman *et al*., 2009b; Lawal *et al*., 2012).

The application of remote sensing in natural disaster management has become common in creating awareness on environmental issues and providing recent imageries to the public. With the boost in technology, there is rise in expectations for latest monitoring and visual imagery to be provided for emergencies and natural disaster management (Ghani *et al*., 2012).

In order to obtain better quality information, images are fused together in a process of combining two or multiple images to obtain more detailed information with the aid of certain algorithms (Ehlers *et al*., 2010). Despite the rapid development of data fusion in the field of remote sensing, multisensor data fusion is still a challenge (Palubinskas *et al*., 2010). Most studies on fusion have been done using different bands of SAR for classification purposes but the TerraSAR-X is a newer data recently applied in a few studies compared to other bands with longer wavelengths. More commonly researchers have worked on fusion of SAR and optical imageries, but little has been done on fusion of different SAR bands, like the TerraSAR-X with RadarSat-1 especially not in the study area.

However fusion of SAR and Optical data is not completely reliable because the possibility of having both remote sensing data (SAR and Optical) is difficult in some cases due to its incompatibility with all weather conditions. On the basis of the quest for more detailed information, the incompatibility of the Optical data makes it worth to compare different types of SAR data in flooded area detection using fusion and classification of images; this is in order to determine whether it is a more appropriate decision to fuse the various bands of SAR data for further flood classification. However, contrary to some recent articles which integrated radar images with multi bands, the goal of this research is to integrate three single band SAR images of different spatial resolutions to investigate their efficacy in improving classification, providing more interpretable information and boundaries that can aid in addressing the flood disastrous challenges in the study area. This can be achieved through the fusion of two Radarsat-1 images and a TerraSAR-X image of the study area and secondly by investigation of a suitable fusion technique for delineation of flooded areas in the study area (Fig. 1).

STUDY AREA

Perlis is an important state of Malaysia located at the northern coast, lying south of the border and Thailand to the north. It covers an area of 795 km^2 of land, with a population of 217,480 making it the smallest state in the country. Annual temperature in Perlis is from 21°C to 32°C while the annual average rainfall is 2000 to 2500 mm.

Kedah is another important state in Malaysia, south of Perlis, located in the northwestern part of peninsular Malaysia, covering a total land area of 9425 km^2 with a population of 2.012 million. The climate of Kedah is a tropical monsoon with a uniform temperature between 21°C and 32°C, with an average annual rainfall between 2032 and 2540 mm.

MATERIALS AND METHODS

The primary satellite images used in this research study includes two RadarSat-1 images of the pre and post periods of flooding in the study area, a TerraSAR-X image of the during flood period. The RadarSat images both have single bands with 25 m resolution, with the RadarSat pre flood having an ascending orbit, while the RadarSat post flood is of a descending orbit. Both have rectified skew orthomorphic projections. The TerraSAR-X image used has a single band with 18 m resolution, captured by a descending orbit (Fig. 2).

Preprocessing: As a result of the antenna gain pattern common in radar**,** the images typically have variation in gain in the opposite direction of the range; antenna

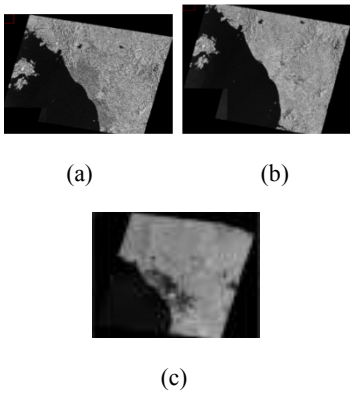

(a) (b)

(c)

Fig. 2: (a): Radarsat 1 before flood; (b): Radarsat 1 after flood; (c): TerraSAR-X during flood

pattern correction was made on the datasets to remove these gains. The antenna pattern correction was done as the first preparatory process before the images were filtered using multiplicative polynomial order 1.The Lee and Frost Filter were used to despeckle the images by smoothing the noise using a default noise variance of 0.2500 and a filter size 3×3, but the Lee Filter was preferred over the Frost because of better appearance of edges and used to smooth the noise in the images that have an intensity which is related to the images based on statistics and it preserved the sharpness of the image while reducing the noise.

In this study image to image registration was used to co register the images at a root mean square error of 0.464514. The three radar datasets which cover most part of the northern states of Malaysia, i.e. Kedah, Perlis, Perak and Penang were acquired in three different periods of march 2010, November 2010 and January 2011, representing periods of before, during and after floods. The data sets were of different sensors; therefore they were co registered to the same geographical reference by image to image registration in ENVI 4.8, which is UTM zone 47 N projections and datum WGS84.

Layer Stacking was done by creating a multiband layer from the three different images which were of different pixel sizes and extent, the individual input bands were resampled using the nearest neighbor to the same pixel size that is the pixel size of the higher resolution TerraSAR-X which is 18 meters. The output band contained all the extent of the three bands and the study area was therefore extracted from the only extent where the three files overlap. The overlapped extent reduced the coverage area to Perlis and Kedah States.

Processing: The images were fused together in combination in order to obtain more reliable and interpretable information. It was done at pixel level using the methods in the following subsections. This was carried out with the aim of achieving a more enhanced and sharpened image by improving the lower resolutions. Four methods of data fusion were used and they include; Hue Saturation Value (HSV), Brovey Transformation (BT), Gram Schmidt Spectral Sharpening (GS) and the Principal Component Spectral Sharpening (PCSS).

Hue, Saturation, Value (HSV): The HSV method separates spectral information into Hue, saturation and value, it is referred to as a method of transforming RGB into color space with the aim of replacing the low resolution band with the high resolution one and resample the hue as well as the saturation bands automatically to the higher resolution pixel size and then finally transform the image back to RGB. This will make the RGB output to have the pixel size of high resolution input data (Jia and Minhe, 2011; ENVI, 2008).

Brovey Transformation (BT): The Brovey transformation method was initially to increase visually the contrast between the two ends of an image histogram that is the high and low ends, thereby changing the original geometry of the scene. This method was developed to produce RGB image which is the reason why only three bands can be merged at a time (Louis *et al*., 2013). It uses mathematical combinations of the images so that the higher resolution will be multiplied by the each of the lower resolution images and is considered appreciable in producing good quality outputs, (Rokni *et al*., 2014).

Gram Schmidt (GS): The goal of GS is to minimize redundancy in the data; it is one of the common techniques in multivariate statistics (Rokni *et al*., 2014). It is a transformation method that uses the higher spatial resolution data to sharpen the lower resolution data by simulating it. It uses the spectral response of a given sensor to determine the look of the panchromatic data, i.e., the way it.

Principal Component Spectral Sharpening (PCSS): This is also another pan sharpening method similar to Gram Schmidt with only a subtle difference in their output and the different technique they use. The main difference between them is that the Gram Schmidt uses spectral response function of the sensor to determine the appearance of the panchromatic band. Their differences can also be seen in their spectral information (spectral profile), (ENVI, 2008). This method can be used in data compression and editing and most especially it can be used in the multi spectral bands to create a new image consisting majority if not all the variance (Louis *et al*., 2013). In the case of this study, all the variance will be contained in the image because the images are exactly three in number.

Edge detection: In this study the Laplacian edge detection filter which is a convolution filter was used with a filter size of 5×5 and it was used because the images involved are radar images. According to ENVI (2008) this type of filter enhances edges in SAR images.

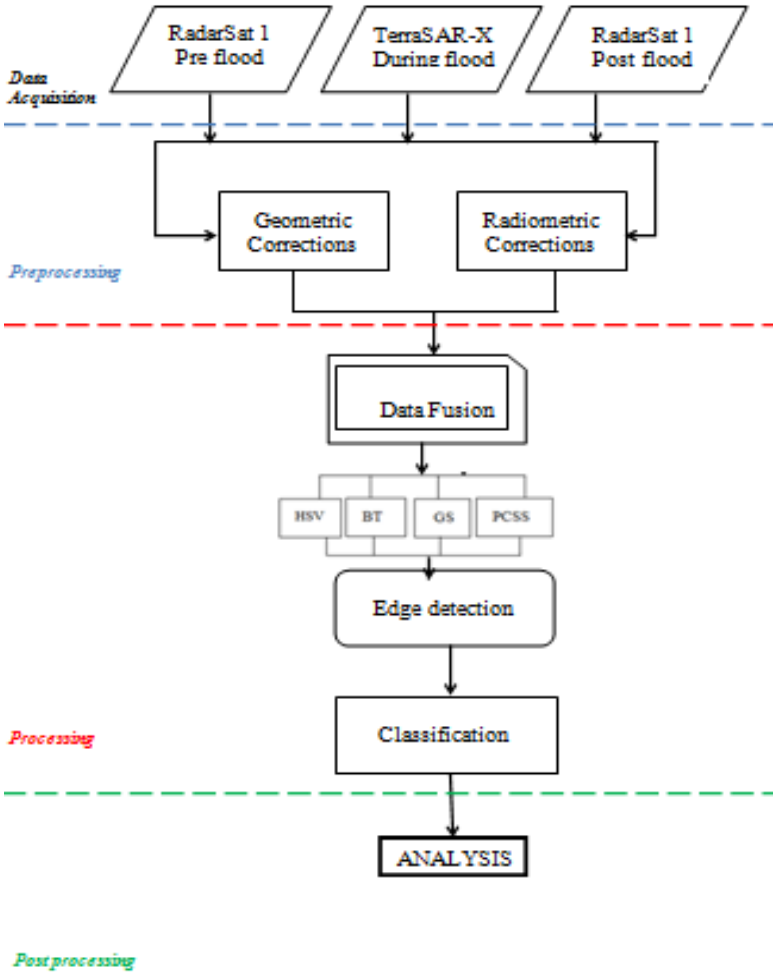

Fig. 3: Flow chart of methodology

Classification: The Supervised Classification was used in this study, which involved the collection of training sites called Region of Interests (ROI). The ROI were selected in two regions namely flooded and none flooded, in order to find out the flood extent of the area regardless of the land use type. The classification was based on all the fused outputs. The two types of classification used in this study are the Maximum Likelihood (ML) and the Support Vector Machine (SVM).

Maximum Likelihood (ML): The Maximum Likelihood (ML) was used to calculate the probability of a pixel occurring in one of each of the two classes (flooded and non flooded). Based on the Gaussian assumption of the ML, i.e., normal distribution, each pixel was allocated to the class in which it has highest probability. The same Region of Interest (ROI) was used in all the outputs of the four methods used.

Support Vector Machine (SVM) The SVM was used to classify all the outputs using the same Region of Interest (ROI). It separated the two classes (flooded and non flooded) by using a gap as a determined surface which divided the classes with the greatest possible difference between them. The ROI were then mapped into predicted classes which they belong (Fig. 3).

RESULT AND ANALYSIS

The preparation of the satellite images was carried out by filtering the images selectively by Lee filter based on clearer observation of the points and the boundaries. After the application of filter, the image statistics improved with decrease in the mean and standard deviations as shown in Table 1.

Figure 4 below, the three images do not completely overlap due to their different sizes; therefore the red box in the figure shows the maximum extent of overlap between the three images that can be used to achieve the objectives of the study, which is to fuse the three images at the same area. All other extents apart from the red box are out of the desired study area, therefore the states of Penang and Perak became outside the study area leaving Perlis and Kedah.

Table 1: Statistical result of the Lee filter of the original images

	Before lee filter				After lee filter			
Satellite images	Min	Max	Mean	S.D.	Min	Max	Mean	S.D.
RadarSat 1 (Preflood)	0	65535	5897	7923	0	62182	5892.7	7494
TerraSAR-X (During flood)	0	18877	80	97	0	17279	80.2637	93
RadarSat 1 (Post flood)	0	65535	5599	7886	0	62194	5595.58	7440

Table 2: Statistical results of Laplacian filter of the fused images

		Laplacian filter			
		Before filter		After filter	
Fused Image	Band	Mean	S.D.	Mean	S.D.
HSV	1	89.25	71.82	82.640	63.36
	2	91.34	78.70	87.420	64.54
	3	87.75	72.17	81.510	63.07
BT	1	82.27	67.39	110.25	54.34
	2	0.000	0.000	253.26	7.970
	3	86.15	68.50	112.11	50.98
GS	1	88.81	64.16	93.390	58.01
	2	83.79	70.32	131.70	45.05
	3	90.42	63.57	97.130	56.35
PCSS	1	89.12	64.04	93.340	57.74
	2	83.81	70.44	132.96	44.97
	3	90.02	63.89	98.200	56.47

S.D.: Standard deviation

Fig. 4: Extraction of the actual study area

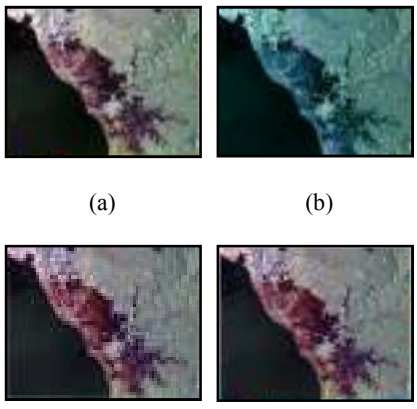

(a) (b)

(c) (d)

Fig. 5: Fusion results; (a): HSV; (b): BT; (c): GS; (d): PCSS

Fusion: In this section, the four pixel based level fused outputs are presented, i.e., the HSV, BT, GS and the PCSS result of fusion. By visually comparing the outputs, they are almost equal in spectral characteristics with only minimal difference.

The HSV fusion output as shown in Fig. 5a showed more contrast between the different parts of the image using the hue (pure color attribute), the saturation (the degree of purity of the color and the value (the intensity) which describes the brightness or dullness. The flooded area in Fig. 5a compared to Fig. 2c of the original TerraSAR-X (during flood) image, shows that the HSV coverage of the area is a similar estimate of the original coverage area.

The BT output in Fig. 5b is visually different from the other fusion methods because the overall image brightness is lower compared to the other fusion outputs, which never the less gave an appreciable vision of the flooded area. This could be as a result of the BT technique of changing the radiometry of the scene (Louis *et al*., 2013) and thereby showing more contrast between the flooded and non-flooded areas.

Similar to the HSV, the GS and PCSS also have color composites that indicate the different spectral characteristics of objects, such as different colors representing different objects and mixtures of different colors meaning mixture of different objects in one place such as mixed land uses. The main difference between Fig. 5a, c and d is that the blue color in the southwestern area is an indication of information presented in the Fig. 5c and d which cannot be seen in the Fig. 5a. On the other hand, the flooded area coverage that can be seen in the HSV is unclear in both the GS and the PCSS.

Edge detection: After the completion of the fusion step in processing, the fused images were all filtered using the Laplacian non directional filter specifically to improve the image edges for classification. The result of the filter was observed in the image statistics as shown in Table 2.

Classification: The classification results includes both Maximum Likelihood (ML) and Support Vector

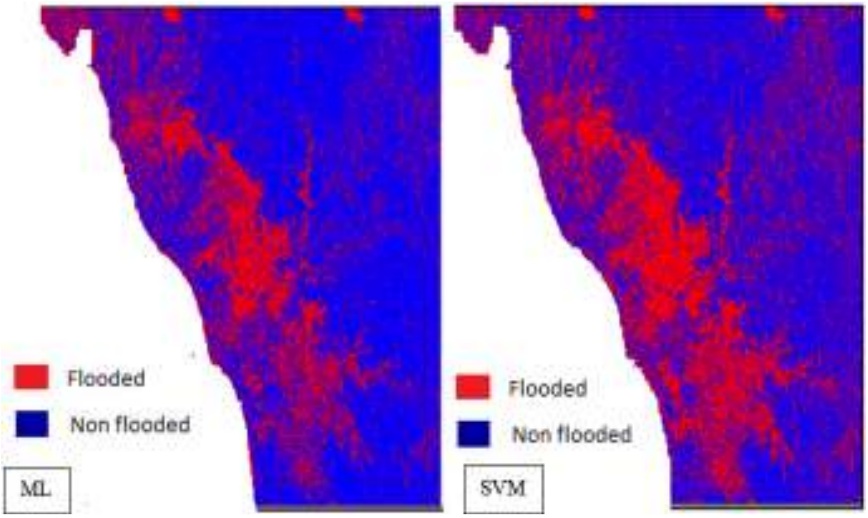
Flooded
Non flooded
ML
Flooded
Non flooded
SVM

(a)

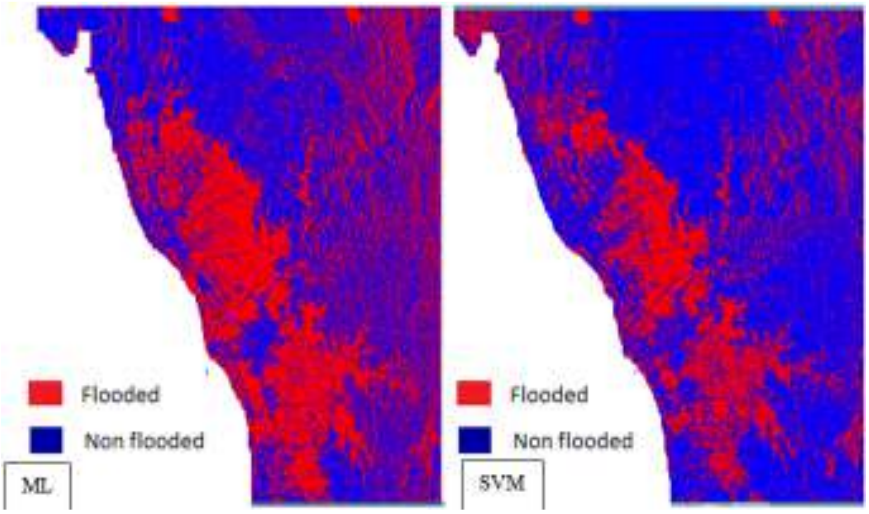
Flooded
Non flooded
ML
Flooded
Non flooded
SVM

(b)

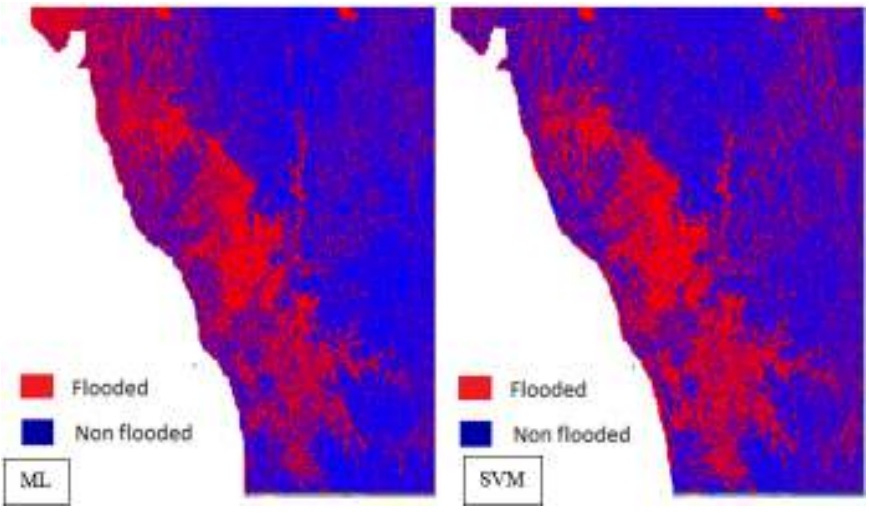
Flooded
Non flooded
ML
Flooded
Non flooded
SVM

(c)

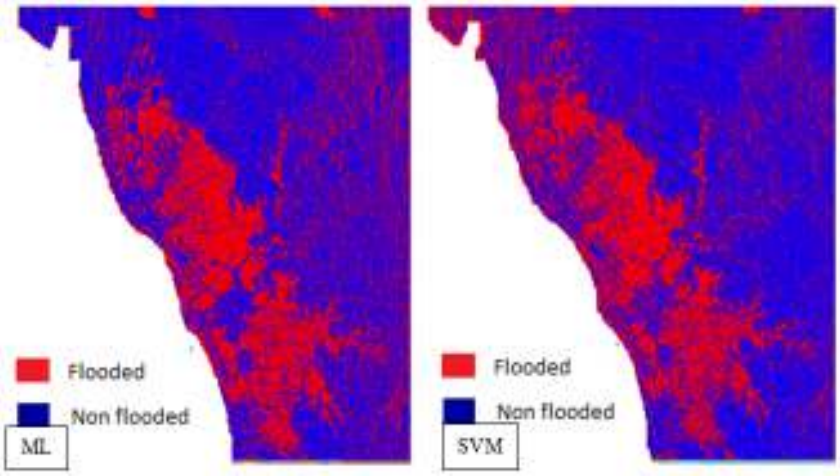

(d)

Fig. 6: Classification outputs of maximum likelihood and support vector machine; (a): GS-ML and GS-SVM; (b): BT-ML and BT-SVM; (c): PCSS-ML and PCSS-SVM; (d): HSV-ML and HSV-SVM

Table 3: Accuracy assessment results

	Maximum likelihood		Support Vector Machine	
Fusion technique	Overall accuracy (%)	Kappa coefficients	Overall accuracy (%)	Kappa Coefficient
PCSS	65.5978	0.2878	70.4047	0.3321
Gram Schmidt (GS)	68.0616	0.3186	70.4041	0.3340
Hue Saturation Value (HSV)	69.7889	0.3012	70.4606	0.3418
Brovey Transformation (BT)	70.1478	0.3179	70.9615	0.3280

Machine (SVM) for each of the technique used as shown in Fig. 6, both put together to compared so that the overall best was selected. With reference to the land use map of the study area, the major constituents were studied to make the interpretation of the classification results easier, by understanding the topography and land use types and distributions within the study area. The major constituents of the study area are paddy and rubber, which covers most proportion of the area, with a part consisting of sugarcane plantation mostly in the north and south, a considerable number of residential areas which are sparsely dispersed but linked by roads and railways.

Figure 6d HSV-ML and HSV-SVM (c) PCSS-ML and PCSS-SVM (b) BT-ML and (a) GS-SVM classified most part of the west coast as flooded which is contrary to the original TerraSAR-X during flood image that shows that part as non-flooded area, but in the Fig. 6a GS-ML and b BT-SVM, the areas classified are closer in extent along the coast. In short, the HSV-ML and HSV-SVM, GS-SVM, BT-ML and PCSS-ML all over classified the paddy in terms of flood extent.

The reclassified land use map was used as a reference to test the accuracies of all the classified outputs in Fig. 6a to d. Table 3 shows the overall accuracies and kappa coefficients of all the methods used in this study.

Based on the accuracy analysis using confusion matrix, Table 3 shows all the overall accuracies and kappa coefficients for all the techniques used. According to the results, the accuracies are very close in values with not much difference between their overall percentage accuracies and kappa coefficient. The BT has the highest accuracy with overall accuracy of 70.9606% and kappa coefficient of 0.3280 for SVM and percentage accuracy of 70.1478% and kappa coefficient of 0.3179 for Maximum Likelihood.

CONCLUSION

The results of this study show the possibility of fusing three different SAR images with single bands, by giving a clearer picture of classification and delineation of the flooded areas. The best among the fusion methods used is the Brovey Transform (BT) method which was validated in the Support Vector Machine (SVM) classification output, using Confusion Matrix with an overall accuracy percentage of 70.9615% and Kappa Coefficient of 0.3280.

ACKNOWLEDGMENT

This study was funded by the Universiti Teknologi Malaysia Research Grant (QJ130000.2527.07H75). We would also like to acknowledge the Malaysian Agency for Remote Sensing for providing the data used in the study.

REFERENCES

Chan, N.W., 2012a. Impacts of Disasters and Disasters Risk Management in Malaysia: The Case of Floods. In: Sawada, Y. and S. Oum (Eds.), Economic and Welfare Impacts of Disasters in East Asia and Policy Responses. ERIA Research Project Report 2011-8, ERIA, Jakarta, pp: 503-551.

Ehlers, M., S. Klonus, P. Johan Åstrand and P. Rosso, 2010. Multi-sensor image fusion for pansharpening in remote sensing. Int. J. Image Data Fusion, 1(1): 25-45.

ENVI, 2008. Guide, E.U.S., 2008. ENVI on-line Software User's Manual. ITT Visual Information Solutions.

FEMA, 2014. Retrieved from: http//www.fema.gov. (Accessed on: March 10th, 2014)

Ghani, A.A., C.K. Chang, C.S. Leow and N.A. Zakaria, 2012. Sungai Pahang digital flood mapping: 2007 flood. Int. J. River Basin Manage., 10(2): 139-148.

Jia, H. and J. Minhe, 2011. Fusion of ALOS and QuickBird imagery for mangrove analysis-A case study in Beilun estuary, Vietnam. Proceeding of 19th International Conference on Geoinformatics, pp: 1-5.

Lawal, D.U., A.N. Matori, A.M. Hashim, I.A. Chandio, S. Sabri, A.L. Balogun and H.A. Abba, 2011. Geographic information system and remote sensing applications in flood hazards management: A review. Res. J. Appl. Sci. Eng. Technol., 3(9): 933-947.

Lawal, D.U., A.N. Matori, A.M. Hashim, K. Wan Yusof and I.A. Chandio, 2012. Detecting flood susceptible areas using GIS-based analytic hierarchy process. Proceeding of International Conference on Future Environment and Energy (IPCBEE), 28: 3-4.

Lawal, D.U., A.N. Matori, K.W. Yusof, A.M. Hashim and A.L. Balogun, 2013. Analysis of the flood extent extraction model and the natural flood influencing factors: A GIS-based and remote sensing analysis. Proceeding of IOP Conference Series: Earth and Environmental Science, 18: 012059.

Louis, R.E., S.K. Mathew, K.G. Puschmann, C. Beck and H. Balthasar, 2013. Formation of a penumbra in a decaying sunspot. Astron. Astrophys., 552: 4.

Palubinskas, G., P. Reinartz and R. Bamler, 2010. Image acquisition geometry analysis for the fusion of optical and radar remote sensing data. Int. J. Image Data Fusion, 1(3): 271-282.

Rokni, K., A. Ahmad, A. Selamat and S. Hazini, 2014. Water feature extraction and change detection using multitemporal landsat imagery. Remote Sens., 6(5): 4173-4189.

Toriman, M.E., A.J. Hassan, M.B. Gazim, M. Mokhtar, S.S. Mastura, O. Jaafar, O. Karim and N.A.A. Aziz, 2009b. Integration of 1-D hydrodynamic model and Gis approach in flood management study in Malaysia. Res. J. Earth Sci., 1(1): 22-27.

Varikoden, H., B. Preethi, A. Samah and C. Babu, 2011. Seasonal variation of rainfall characteristics in different intensity classes over Peninsular Malaysia. J. Hydrol., 404(1): 99-108.